MECHANIKA TEORETYCZNA
I STOSOWANA
Journal of Theoretical
and Applied Mechanics
1, 30, 1992

MODELLING OF RATE–OF–CLIMB INDICATOR DYNAMICS

JERZY GAŁAJ

Warsaw University of Technology

A model of rate-of-climb indicator dynamics (eg. WR-30) has been presented. Physical and mathematical models of an instrument were determined. A digital simulation of proposed model was carried out. The conclusions were formulated on a basis of results obtained during simulation experiments.

List of symbols

- $\delta, \dot{\delta}$ – angular displacement and velocity of output axis [rad, rad/s],
- $w_p, \dot{w}_p$ – displacement and velocity of the centre of differential aneroid [m, m/s],
- q – pressure difference of aneroid [N/m^2],
- V_p – airplane vertical velocity (climb at $V_p < 0$ and descent at $V_p > 0$) [m/s],
- H – altitude [m],
- t_k – temperature inside capillary [°C].

1. Introduction

A main application of a rate–of–climb indicator is the measurement of an airplane vertical velocity. The velocity direction is also pointed out by the instrument. The information about change in the altitude (climb or descent) is given to the pilot.

A basic element of rate–of–climb indicator is a differential aneroid. A deflection of the aneroid centre is approximately proportional to the pressure difference (input signal). The linear motion of the aneroid centre is transformed into rotation of the output axis by means of a crank mechanism. Finally the angular motion of a measurement axis (fixed with indicating needle of the indicator mounted in cockpit) is obtained by means of a gear (sector and pinion).

Rate–of–climb indicators have different measurement ranges bounded within the values 10 m/s ÷ 300 m/s (eg. WAR-300).

The investigation of variometer dynamics as well as the construction of a simple digital model (which can be applied to a flight simulator after some modification) were the main purposes of this paper.

On the basis of functional scheme of variometer and some preliminary assumptions, the physical model of the instrument was derived in the first chapter of the paper. Consequently the mathematical model was formulated in the next step. It contains equations describing either the aneroid and transmission system motions or the pressure difference q. The equations were expressed in the form of a set of first order differential equations (the state equations).

Simulation results for the digital model together with the description of it were presented in the next chapter. The model has taken a form of a computer program written in Turbo Pascal and tested on IBM PC/XT. The variometer indications during two different variants of airplane longitudinal motion were obtained as a result of simulation experiments. The conclusions relating to the model structure and character of indications were formulated in the same chapter.

Final remarks were included in the last chapter.

2. Physical and mathematical model of variometer

The variometer construction and principle of operation have been described for example in [1,3] and [4].

The functional scheme of typical instrument with uniform scale is shown in figure 1.

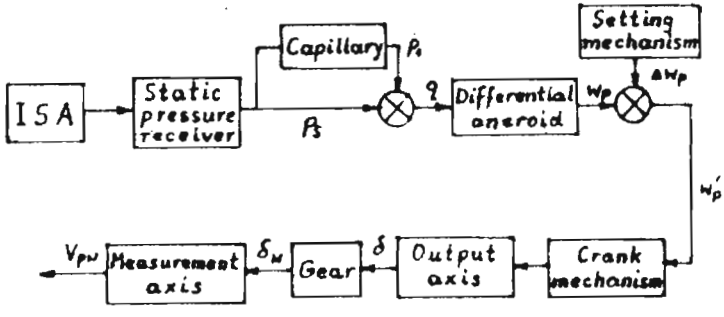

Fig. 1. Functional scheme of variometer with uniform scale

The following preliminary assumptions were employed to define a physical model of variometer:

1. Static pressure and air temperature at altitude H correspond to ISA (International Standard Atmosphere).
2. The centre of aneroid moves along the line perpendicular to the pedestal.
3. The crank mechanism and the sector are balanced statically with regard to the output axis.
4. Deviation inertial moments, aneroid hysteresis and backlashes in mechanical mechanisms are neglected.
5. A temperature inside the instrument is constant and equal to 20°C.
6. A temperature inside capillary is equal to an arithmetic mean of temperatures outside the plane and inside the instrument.
7. Dynamical viscosity of the air inside capillary is a linear function of temperature t_k.

The following cartesian coordinate systems were constituted to obtain mathematical model of variometer

a) $O_g x_g y_g z_g$ – gravitational fixed with airplane,
b) $Oxyz$ – fixed with plane symmetry axes,
c) $O_p x_p y_p z_p$ – fixed with aneroid,
d) $O_k x_k y_k z_k$ – fixed with output axis.

The equations of the aneroid and output axis motions in coordinate systems mentioned above have been derived on the basis of classical mechanics law and physical model presented above. The following mathematical model of a measurement variometer system, written in the form of vector state equation, has been obtained after some arithmetic transformations

$$\dot{\boldsymbol{x}} = \mathbf{A}\boldsymbol{x} + \mathbf{B}\boldsymbol{u} + \mathbf{C} \tag{2.1}$$

where

$$\boldsymbol{x}^{\mathsf{T}} = [\delta, \dot{\delta}, w_p, \dot{w}_p, q]$$
$$\boldsymbol{u} = V_p$$

$$\mathbf{A} = \begin{bmatrix} 0 & 1 & 0 & 0 & 0 \\ a_{21} & a_{22} & a_{23} & 0 & a_{25} \\ 0 & 0 & 0 & 1 & 0 \\ a_{41} & a_{42} & a_{43} & 0 & a_{45} \\ 0 & 0 & 0 & 0 & 1 \end{bmatrix}, \quad \mathbf{B} = \begin{bmatrix} 0 \\ 0 \\ 0 \\ 0 \\ b_5 \end{bmatrix}, \quad \mathbf{C} = \begin{bmatrix} 0 \\ c_2 \\ 0 \\ c_4 \\ 0 \end{bmatrix}.$$

The elements (entries) of matrices **A**, **B** and **C** are the functions of

a) mass, geometric and kinematic parameters of the aneroid and transmission system ($a_{21}, a_{22}, a_{23}, a_{25}, a_{41}, a_{43}, c_2, c_4$),

b) kinematic parameters of the plane (c_2, c_4),

c) geometric parameters of the capillary and instrument housing as well as environment parameters (a_{55}, b_5).

The expressions describing above coefficients have not been enclosed here to make the paper more clear and understandable.

They can be found in [2]. The values of mathematical model parameters were determined considering the data included elswhere [1,4].

3. Digital simulation of a variometer model

A construction of digital model of the instrument has been the next step of modelling process. Diagrams of algorithms of main program and procedures for calculating of differential equations have been depicted. The program in Turbo Pascal has been written on a basis of the algorithms. It has been tested on IBM PC/XT. Two theoretical models of longitudinal motion have been applied for simulation investigations. Climb with velocity 50 m/s as the first variant and descend with velocity 70 m/s as the second variant have been assumed in the simulation model (changes of vertical velocity in time for first and second variant respectively are shown in figures 2 and 3 – broken lines).

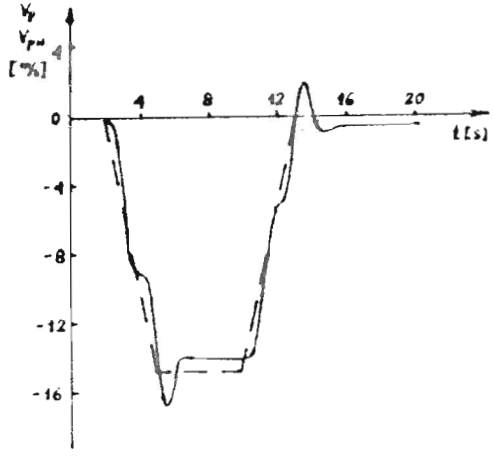

Fig. 2. Indications of variometer model V_{pw} and plane vertical velocity V_p during first variant of flight (climb)

The simulation program enables the following choices

a) one of two variants of flight ($WR = 1$ or 2),

b) integration time t_c, integration step t_i and output step t_w,

c) output mode
   - monitor ($WK = 1$),
   - hard disk ($WK = 2$),
   - printer ($WK = 3$),
   - hard disk and printer ($WK = 4$).

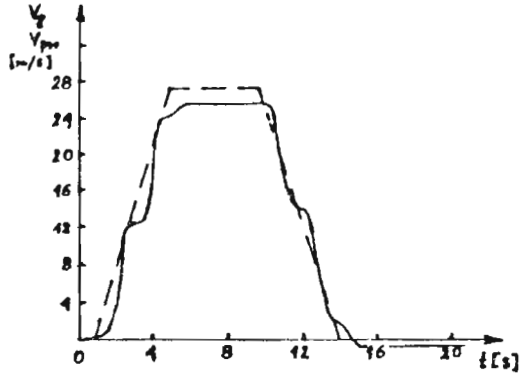

Fig. 3. Indications of variometer model V_{pw} and plane vertical velocity during second variant of flight (descent)

The following time characteristics have been obtained during digital modelling

a) vertical displacement of the aneroid centre $w_p(t)$,

b) angle of rotation of output axis $\delta(t)$,

c) indications of vertical velocity V_{pw},

d) deviations of vertical velocity indications $\varepsilon = V_p - V_{pw}$.

The indications of variometer digital model as well as real vertical velocity as function of time are drawn in Fig.2 (first variant of flight) and Fig.3 (second variant of flight). Adequate deviations of indications are shown in Fig.4 and Fig.5.

The following conclusions have been formulated after analysis of the simulation results

1. Variometer indications follow changes in a vertical velocity during two tested flights including climb ($V_p < 0$) and descent ($V_p > 0$).

2. Deviation of indication ε is time variable. The absolute value of deviation does not exceed the value of: 3 m/s in first flight (climb) and 4 m/s in second

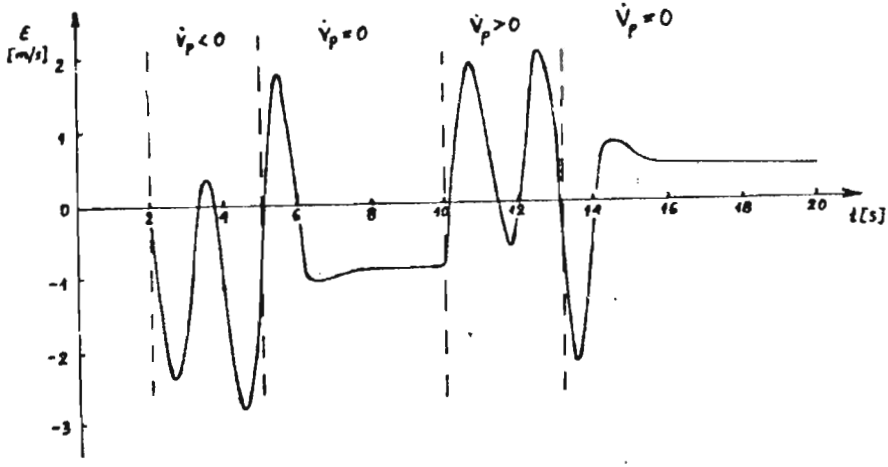

Fig. 4. Deviation of indication of variometer model during first flight

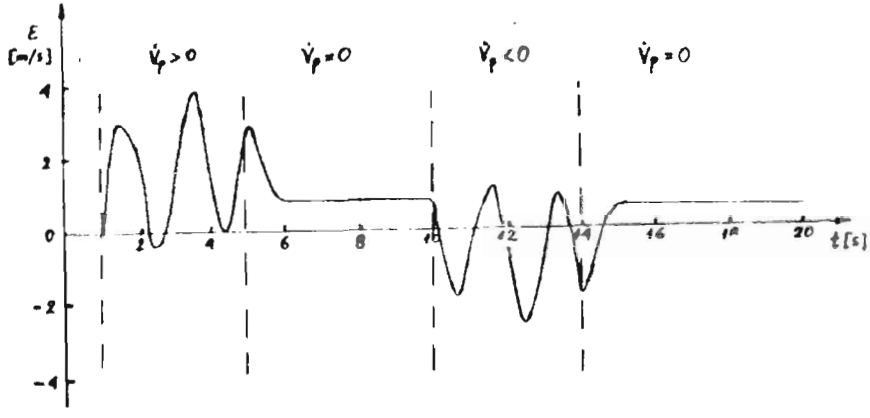

Fig. 5. Deviation of indication of variometer model during second flight

flight (descent). The value of deviation is less then 1 m/s during the flight with constant vertical velocity.

3. Delay of the variometer model indication is less then 1 s.

4. Some differences in variometer indications during two variants of flight can be noticed. A single oscillation appears only during climb (amplitude of oscillation does not exceed 2 m/s).

4. Final remarks

The convergence of model and real instrument indications has been shown by means of a digital simulation. Digital model of the variometer presented here could be used in a flight simulator system provided that faster computer or/and compilator eventually hardware solution would be applied.

References

1. *Membrane instruments*, MON, Warsaw 1968 (in polish)
2. GAŁAJ J., *General model of flight simulation – digital simulation of variometer for application in flight sumulator*, Report 150/88, ITLiMS, Warsaw 1988 (in polish)
3. MICHAJLOV O.M., *Flight instruments*, Maszinostrojenije, Moscow 1964 (in russian)
4. BRASLAVSKIJ D.A., *Flight instruments*, Maszinostrojenije, Moscow 1964 (in russian)
5. ANDRIEJEVA L.E., *Elastic elements of instruments*, Maszgiz Ed., Moscow 1962 (in russian)

Streszczenie

W pracy modelowano własności dynamiczne klasycznego wariometru lotniczego z równomierną skalą (np. typu WR-30). Podczas badań symulacyjnych otrzymano m.in. przebiegi wskazań przyrządu dla kilku wariantów ruchu podłużnego samolotu (wznoszenie i opadanie). Na podstawie wyników modelowania cyfrowego sformułowano szereg wniosków dotyczących charakterystyk pomiarowych wariometru.

Praca wpłynęła do Redakcji dnia 14 czerwca 1988 roku